

PREDICTION OF UNSTABLE REGIMES IN THE OPERATION OF BAGASSE FIRED FURNACES

Peter WOODFIELD¹, John KENT¹, Vasily NOVOZHILOV¹ and Terry DIXON²

¹ Department of Mechanical and Mechatronic Engineering, The University of Sydney, NSW 2006, AUSTRALIA

² Sugar Research Institute, 239-255 Nebo Rd., Mackay, QLD 4740, AUSTRALIA

ABSTRACT

Combustion stability in bagasse fired furnaces, which is caused by periodic particle deposit and burn-out on the grate of the furnace, is investigated using Computational Fluid Dynamics (CFD) approach. The grate is modeled as a packed bed with momentum and heat transfer equations being solved to describe particle drying and combustion in the stream of undegrated air. Combustion of the bed is modeled via a first order Arrhenius reaction scheme.

The grate model is incorporated into a three-dimensional, time-dependent CFD predictions of reactive flow inside the furnace which includes radiation and bagasse particulate burning.

Predicted transition between stable and oscillating regimes is in reasonable agreement with the measurements. The frequency of oscillations in the exit oxygen concentration in an unstable regime is successfully predicted. This frequency depends on the rates of particle drying and combustion, and corresponds to the periods of complete particle bed burnout.

NOMENCLATURE

A	pre-exponential factor
A_d	particle projected area
C_d	drag coefficient
c_g	gas specific heat
E	activation energy
\mathbf{g}	gravity vector
h	bagasse pile height
h_{fg}	latent heat of water evaporation
k	reaction rate coefficient
M	bagasse surface density on the grate
m_w	water evaporation rate
q_{rad}	radiation flux to particle
q_{cond}	conduction heat flux to particle
S_ϕ	source terms for variable ϕ
$S_{p\phi}$	source terms for variable ϕ due to particles
t	time
T	temperature
T_p	particle temperature
T_∞	free stream temperature
U	gas velocity
V	particle velocity
x, y, z	cartesian coordinates
$Y_{w,s}$	water vapour mass fraction at the particle surface

$Y_{w,\infty}$	water vapour mass fraction in free stream
ρ	density
μ	dynamic viscosity
v	bed void fraction
η	mass of volatiles released divided by the original dry mass
η^*	ultimate mass of volatiles released divided by the original dry mass
Ω	packing density

INTRODUCTION

Bagasse fired furnaces and boilers are widely used in the sugar processing industry. Combustion stability, essential for effective operation of these devices, is largely undermined, however, by periodic particle deposit and burn-out on the grate of the furnace.

There have been a number of CFD studies concerned with flow predictions in bagasse fired furnaces. Luo and Stanmore (1994) compared predictions of temperature, oxygen concentrations and wall heat fluxes with the measurements taken at steady-state conditions. Further comparison between numerical predictions and temperature measurements inside furnace have been provided by Woodfield et al. (1997). Woodfield et al. (1998) investigated the effect of fuel moisture on the combustion stability in the furnace. It has been demonstrated that the CFD modeling can predict a critical bagasse moisture where, for a given set of conditions, ignition becomes unstable.

Measurements of carbon monoxide and oxygen during cycling behavior of the furnace have been performed by Dixon (1983) who observed continuous cycling for operating periods of 2 - 8 hours. He found that uniform bagasse distribution is essential for stability. Generally, a primary source of instability is a high moisture content of the fuel which causes an ignition delay. This results in bagasse accumulating on the grate, drying and burning in a periodic manner. The problem aggravates if non-uniform supply occurs from the bagasse feeders and distributor pressure is not adequate. Under such conditions, combustion cycling can take place over the majority of the grate area and bagasse deposits higher than 1 m are common (Dixon, 1983).

Modeling of unstable regimes is more complicated than the steady-state furnace modeling since an additional submodel is required to take into account the grate effects, such as accumulating and burning. The first attempt has been made by Woodfield et al. (1999) who modelled the grate pile as a two-dimensional packed bed, so that the properties of a bagasse pile were assumed uniform in the vertical direction. The burning rate has been assumed to be constant in time, independent of the bagasse pile properties.

In order to predict instabilities a more realistic model of the grate burning is required. In the present study, the grate is modeled as a three-dimensional packed bed, which

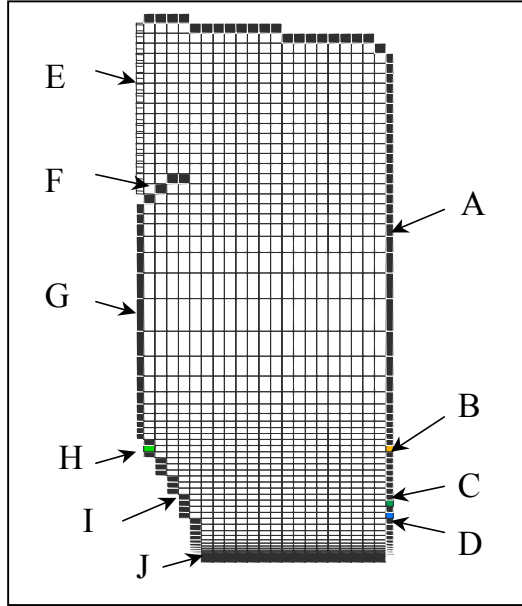


Figure 1: Computational grid for Pleystowe No. 2 Bagasse fired furnace. A: Furnace front wall, B: Secondary air, C: Bagasse spreader, D: Secondary air, E: Furnace outlet, F: Baffle, G: Back wall, H: Secondary air, I: Sloping back wall, J: Grate

allows the properties variation across the bed thickness to be considered. The burning rate modeling is based on experimentally verified bagasse particle kinetics.

FURNACE OPERATING CONDITIONS

Pleystowe No. 2 (Mackay, Queensland) operates at a nominal power of 109 MW. The bagasse distributors are spaced evenly in a horizontal line on the front wall of the furnace 2.0 m above the grate. Two secondary air fans provide secondary air at both the front and rear of the boiler.

The furnace is 18.3 m high, 9.46 m wide and 7.56 m deep. The geometry of the furnace and the grid (consisted of 22,848 cells) used in computations are shown in Fig. 1. Due to symmetry, only half of the furnace needs to be modeled.

The two major operating parameters are air flows into the furnace and the bagasse supply rate. These parameters have been calculated using the flue gas oxygen concentration via stoichiometry and an energy balance over the entire furnace. Three cases are considered in the

present study, namely the low (case (a)), normal (case (b)) and high (case (c)) bagasse loadings. Under the usual operational practice the under-grate air flow increases with the bagasse loading.

The operating conditions and properties of the fuel are summarized in Table 1.

C (% dry ash free)	50.51
H (% daf)	6.31
N (% daf)	0.12
O (% daf) (by difference)	43.06
H ₂ O (% wet)	51.0
Ash (% dry)	5.75
Fuel Specific Energy (HHV) (kg/kg daf)	19554.
Bagasse Flow (kg/s wet) – case (a)	13.51
Bagasse Flow (kg/s wet) – case (b)	19.3
Bagasse Flow (kg/s wet) – case (c)	28.95
Under-grate air (kg/s) – case (a)	29.05
Under-grate air (kg/s) – case (b)	49.9
Under-grate air (kg/s) – case (c)	84.7
Front secondary air (kg/s)	6.0
Rear secondary air (kg/s)	9.5
Distribution air jets (kg/s)	2.4
Distribution secondary air (kg/s)	1.7
Furnace wall temperature (K)	477
Fuel packing density (kg/m ³ dry)	60
Pile voidage (m ³ /m ³)	0.8
Pile internal surface area (m ² /m ³)	160
Critical pile moisture (%)	15
Characteristic particle size for grate (mm)	2.4

Table 1: Furnace operating conditions

CFD Model of the Furnace

The *FURNACE* computational model by J.H.Kent, University of Sydney (Boyd and Kent, 1986; Mann and Kent, 1994) is used. The code solves three-dimensional Favre-averaged equations for weakly compressible flow of the form

$$\frac{\partial(\rho\phi)}{\partial t} + \nabla \cdot (\rho\bar{U}\phi) = \nabla \cdot (\Gamma_{\phi} \nabla \phi) + S_{\phi} + S_{p\phi} \quad (1)$$

Turbulence closure is achieved via the conventional $k - \epsilon$ model with the necessary modifications to account for additional turbulence production due to buoyancy. Additional equations are solved for the mixture fraction and its variance (which serve to implement a fast chemistry PDF combustion model), and evaporated water vapour mass fraction. Radiation transfer is modeled via the Discrete Transfer Method.

Bagasse particles are tracked using a Lagrangian equation of motion

$$m_p \frac{d\vec{V}}{dt} = \frac{1}{2} A_p C_d \rho (\vec{U} - \vec{V}) |\vec{U} - \vec{V}| + \vec{g} \quad (2)$$

in order to obtain particle trajectories. The drag coefficient for bagasse particles is based on measurements by Nebra and Macedo (1988). It is close to, but somewhat lower than the empirical correlation for cylindrical particles (Clift, et al., 1978).

The drying model for the entrained particles is based on Spalding's B-number approach (Kuo, 1986). Conservation of energy gives the thermal B-number

$$B_T = \frac{c_g (T_\infty - T_p)}{h_{fg} - \frac{(q_{rad} - q_{cond})}{m_w}} \quad (3)$$

and conservation of species involves the transport B-number

$$B_D = \frac{(Y_{w,\infty} - Y_{w,s})}{Y_{w,s} - 1} \quad (4)$$

Assumptions of a unity Lewis number ($B_T = B_D$) and uniform temperature distribution inside the particle leads to an equation which may be solved to determine particle temperature along the trajectory. The heat transfer coefficient is determined using a correlation for small cylindrical particles in suspension. The mass fraction of vapour at the particle surface is assumed to be in a local saturated equilibrium.

Particle burning is assumed to start when the particle is completely dry. Devolatilization of combustibles is modeled using single step Arrhenius form equations (Woodfield et al., 1999). Char combustion is modeled using the coal-char model of Smith (1982), with char combustion kinetics determined by Luo and Stanmore (1994), for bagasse.

Grate Model

The pile of bagasse particles accumulating on the grate is considered as a three-dimensional packed bed with the thickness varying with time and location. The pile occupies a few layers of computational cells at the bottom of the furnace.

Generally, the thickness of the pile accumulating on the grate is small compared with the furnace dimensions. For most operating conditions, the pile height does not exceed 20 – 30 cm. Particles are relatively loosely packed as they fall on the grate and are not subjected to any additional compression.

At a particular location, the pile height is updated at each time step taking into account the number of particles falling on the grate per unit time and the particle burning rate. The height of the pile is calculated using the specified packed density as

$$h(x, y, t) = \frac{M(x, y, t)}{\Omega} \quad (5)$$

The height $h(x, y, t)$ determines the actual number of cells in the vertical direction occupied by the pile at a given location on the grate (Fig. 2).

There may be several approaches to the modeling of physical processes inside the grate pile. In some investigations (Fatehi and Kaviany, 1994) the gas-particle system is modeled as a single continuum with unified characteristics (such as temperature). The approach taken

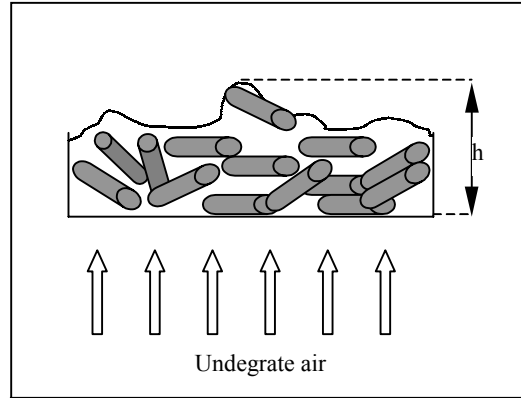


Figure 2 Sketch of flow configuration through the pile

in the present study, treats the bagasse pile as a two-phase system. Because of the loose packing, direct heat exchange between the solid particles (except for radiation) is neglected. The particles, however, exchange heat, mass and momentum with the air stream. As a result of this

exchange, there is also an implicit interaction between the different particles via the gas phase.

Such an approach results in a unified computational arrangement for gas-solid interaction for both moving bagasse particles, and the particles lying in the bed. In the latter case the particulate phase is not disperse, however, the computations can be carried out in essentially Lagrangian manner using the heat/mass transfer correlations, suitable for packed beds.

The drying model for the bed is similar to that described by equations (3) and (4) with the exception that the heat transfer coefficient is taken from the correlation for a packed bed (Incropera and DeWitt, 1996).

$$Nu = Re \cdot Pr^{1/3} \cdot \frac{2.06 Re^{-0.575}}{v} \quad (6)$$

The Reynolds number calculation is based on the characteristic particle size in the pile which is introduced as an input empirical parameter.

Visual observations show that ignition of the pile happens as a result of burning particles falling on the grate which give rise to local hot spots. The pile should be sufficiently dry in order to ignite. It is assumed in the computations that ignition happens if the average moisture in the pile falls below some critical level. Ignition is assumed to happen at the top of the pile.

Combustion of bagasse is modeled via the following Arrhenius kinetic mechanism

$$\frac{d\eta}{dt} = k(\eta^* - \eta) \quad (7)$$

following the work by Drummond and Drummond (1996).

Here η is the mass of volatiles released divided by the original dry sample mass, η^* is the ultimate mass of

volatiles released divided by the original dry sample mass, and k is the Arrhenius rate coefficient given by

$$k = A \exp\left(\frac{-E}{RT}\right) \quad (8)$$

The kinetic parameters were taken as follows (Drummond and Drummond, 1996) : $A = 2.13e6$ (s^{-1}); $E = 92.6$ (kJ/mol).

The top surface of the pile is subjected to a radiation flux, which is obtained from the radiation model. Radiation exchange between layers in the pile is modeled using the bagasse particle temperatures and emissivity.

RESULTS

Steady-state solutions for all the cases ((a), (b) and (c)) are obtained first, and then the corresponding unsteady solutions are computed for the period of 300 s. The time step used in the calculations is 3 s. The critical moisture content used as an ignition criterion is set to 15%.

Pile build-up is controlled by the dynamics of different groups of particles in the flow. The pile of bagasse particles consists of relatively large particles which fall on the grate due to gravity, while lighter particles are carried upwards by undergrate and secondary air currents (Fig. 3). Most falling particles are accumulated close to the back wall of the furnace.

At each location on the grate, the pile undergoes stages of accumulation, drying and combustion. Successive repetition of these stages results in the oscillating behavior of the furnace.

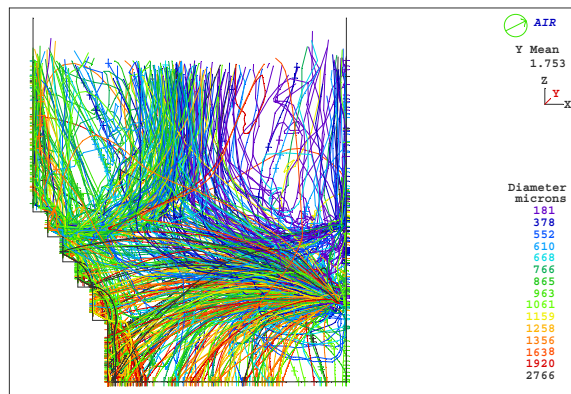


Figure 3 Particle trajectories in the lower part of the furnace

The grate pile does not burn uniformly, and flame may exist at some locations, while the bagasse undergoes drying in other parts on the grate. This result in a rather random flame shape in the lower part of the furnace. As an illustration, the temperature contours are shown in Fig. 4

and 5 at different times during operation. For the first case (Fig. 4) almost the whole grate area is involved in combustion, with the exception of the region close to the

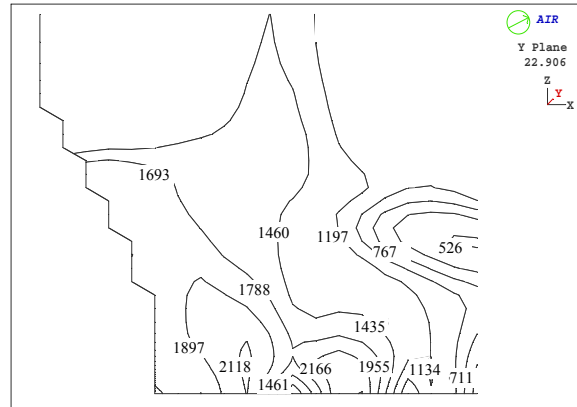


Figure 4 The temperature distribution in the lower part of the furnace for case (b) at $t = 229$ s.

front wall, which is not sufficiently fed with the fuel (Figure 3).

In the other case (Fig. 5), combustion is restricted to the three narrow spots, spaced approximately equally through the grate area.

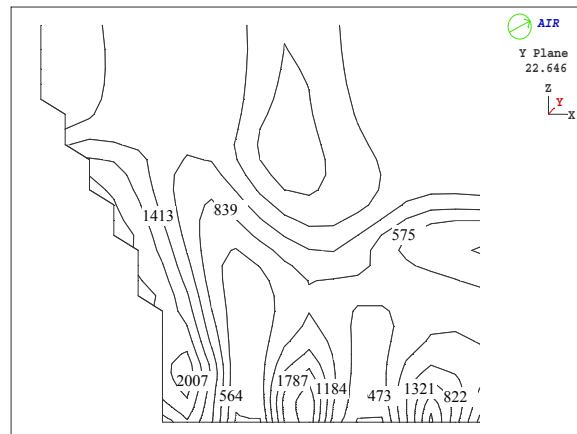


Figure 5 The temperature distribution in the lower part of the furnace for case (b) at $t = 234$ s.

The overall influence of the grate on furnace behavior is determined by the processes in the pile at different locations. These processes are basically determined by the competition between the three rates: (i) the rate of fuel supply (which is determined by the global flow in the furnace), (ii) the rate of drying, and (iii) the rate of burning.

The experimental observation of Dixon (1983) may be interpreted on the basis of comparison of the above rates.

The furnace operation is stable if the fuel supply rate is low (below the normal operating conditions). In this case the falling bagasse dries up and burns quickly. The pile cannot achieve a significant height, and only a thin layer of fuel accumulates.

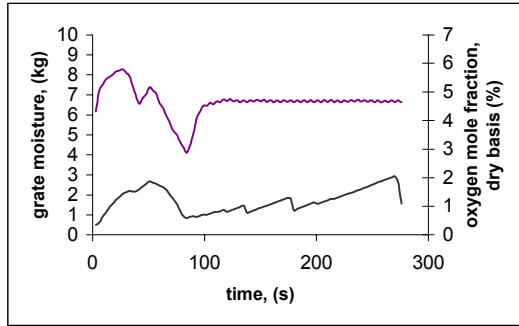


Figure 6 Grate moisture content (bottom) and flue gas oxygen mass fraction (top) for case (a). Bagasse loading is 70% of the normal operating conditions.

At higher bagasse supply rates there is a significant delay in the drying. Particles continue to fall on the grate while the bottom layers start to dry in the undergrate air stream. It should be noted that the under-grate flow rate increases with the bagasse loading which enhance the air stream drying capability. Eventually the moisture in the pile falls below the critical level, and combustion starts. These events lead to the oscillating behavior of the furnace.

To quantify the transition between the stable and unstable regimes, three cases with the different bagasse supply rates (and different under-grate air flow) were considered in the computations. Unstable combustion on the grate manifests itself through fluctuations in the flue gas oxygen concentration, making the latter a convenient parameter for the analysis.

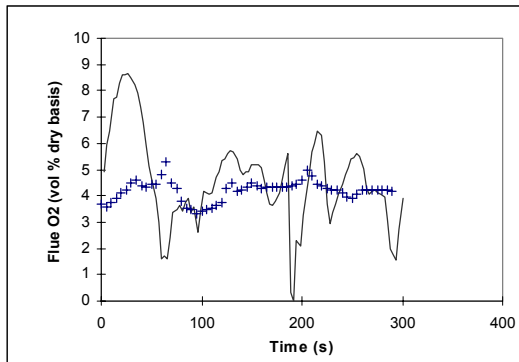


Figure 7 Flue gas oxygen concentration for the normal operating conditions (case (b)).

— calculations
+ measurements

Low bagasse loading is represented by the case (a). The fuel supply rate is about 70% of that at the normal operating conditions. The computed oxygen concentration in the flue gas is presented in Fig. 6. The concentration becomes very stable at about 4.5% after some initial transition period.

This is consistent with the observations. The level of oxygen concentration is also in a good agreement with the measurements.

Case (b) represents the normal operating conditions. The experimental measurements are taken from the study by Dixon, 1983. The measured values are still relatively stable, but give some indication of transition to instability via the development of small oscillations. No distinctive pattern is observed for these fluctuations. CFD calculations are much less stable for this case than for the case with 70% bagasse loading (Fig. 6). The amplitude of fluctuations is definitely higher in the calculations. However, after the initial transition period (of about a minute), they have the same mean value as the experimentally observed oxygen level. The point there the oxygen concentration reaches zero, corresponds to rapid burning of the pile.

Fully developed cycling behavior is observed for high (150% of the normal) bagasse loading. The measured oxygen concentration have a clear oscillating pattern with the period of about 80 s (Dixon, 1983). The cycling of the oxygen concentration from 2.5 % to 5.5 % is typical.

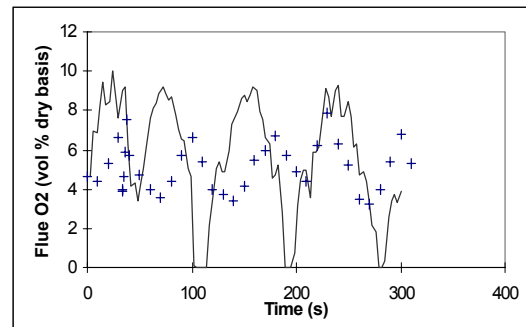


Figure 8 Flue gas oxygen concentration for the high bagasse loading (case (c)).

— calculations
+ measurements

The oscillating nature of the solution is also obvious in the CFD simulation (Fig. 8). The model, therefore, predicts the transition to instability which results from the change in operating conditions.

The frequency of oscillations is reasonably well predicted by the simulations in this case. Maximum values of oxygen concentration are also close to the measured ones, although at some peaks they are about 1.5 times overpredicted. The difficulty is in the prediction of the

minimum concentrations. In the calculations, this value reaches zero, which is an indication of the burning rate overprediction. This may be attributed to the uncertainty in the bagasse kinetic parameters. The latter are still not well-established and the values suggested by different investigators (Drummond and Drummond, 1996; Stubington and Aiman, 1994; Aiman and Stubington, 1993; Luo, 1993) have significant discrepancies. This makes the establishment of the detailed combustion model difficult.

In order to test grid independence the grid was refined up to 26,560 cells. The runs with the refined grid gave a very similar results for temperature distributions and frequency of oscillations.

Woodfield et al. (1999) have shown that it is possible to match experimental observations quite well by adjusting the arbitrary chosen constant burning rate of the pile. It is obviously desirable to adapt the present approach to the more realistic modeling of the pile combustion. The model presented in the present paper is based on more realistic considerations. The model predicts the main features of the furnace behavior at different operating conditions. However, further refinement of the present model is needed to improve the quality of predictions.

CONCLUSION

Combustion instabilities in bagasse fired furnaces have been predicted using a CFD model for grate combustion. Instabilities have been shown to occur at high bagasse loadings. The transition between stable and unstable regimes is determined primarily by the competition between the fuel supply rate and the drying rate of the bagasse particles. The frequency of oscillations is determined by both the drying and burning rate of the particles on the grate.

The predicted frequency of oscillations and maximum values of the flue gas oxygen concentration are generally in reasonable agreement with the measured values. The minimum oxygen level is under-predicted in computations which suggests that the computed burning rates are higher than those measured in the reality. Improvements in the kinetics modeling is required to improve the quality of predictions.

REFERENCES

- AIMAN, S. and STUBINGTON, J.F. (1993) "The pyrolysis kinetics of bagasse at low heating rates", *Biomass and Bioenergy*, 5:113 – 120.
- BOYD, R.K. and KENT, J.H. (1986) "Three-dimensional furnace computer modeling", *21st Symposium (International) on Combustion*, The Combustion Institute, 265 – 274.
- DIXON, T. F. (1983) "Combustion characteristics of bagasse suspension boilers", *Proceedings of Australian Society of Sugar Cane Technologists*, 265 – 271.
- DRUMMOND, A.F. and DRUMMOND, I.W. (1996) "Pyrolysis of sugar cane bagasse in a wire-mash reactor", *Ind. Eng. Chem. Res.*, 35:1263 – 1268.
- FATEHI, M. and KAVIANY, M. (1994) "Adiabatic reverse combustion in a packed bed", *Combustion and Flame*, 99:1 – 17.
- INCROPERA, F.P. and DeWitt, D.P. (1996) "Fundamentals of Heat and Mass Transfer", John Wiley & Sons, New York.
- KUO, K.K. (1986) "Principles of Combustion", John Wiley & Sons, New York.
- LUO, M. and STANMORE, B.R., (1994) "Modeling combustion in a bagasse-fired furnace 1: Formulation and testing of the model", *Journal of the Institute of Energy*, 67, 128 – 135.

MANN, A.P. and KENT, J.H. (1994) "A computational study of heterogeneous char reactions in a full-scale furnace", *Combustion and Flame*, 99: 147-156.

NEBRA, S.A. and MACEDO, I.C. (1988) "Bagasse particles shape and size and their free-settling velocity", *Int. Sugar Journal*, 90(1077), 168 – 170.

SMITH, I.W. (1982) *Nineteenth Symposium (International) on Combustion*, The Combustion Institute, Pittsburgh, 1045 – 1065.

STUBINGTON, J.F. and AIMAN, S. (1994) "Pyrolysis kinetics of bagasse at high heating rates", *Energy and Fuels*, 8:194 – 203.

WOODFIELD, P.L., KENT, J.H. and DIXON, T.F. (1997) "Temperature measurements in a Bagasse-Fired Furnace – Experimental and Numerical results", *Proceedings of Australian Society of Sugar Cane Technologists*, 19, 473 – 478.

WOODFIELD, P.L., KENT, J.H. and DIXON, T.F. (1998) "Computational modeling of a Bagasse-Fired Furnace – Effects of moisture", *Proceedings of Australian Society of Sugar Cane Technologists*, 19, 473 – 478.

WOODFIELD, P.L., KENT, J.H. and DIXON, T.F. (1999) "Computational modeling of combustion instability in bagasse fired furnaces", *The Combustion Institute, Mediterranean Combustion Symposium*, Antalya, Turkey, June, 813 – 824.